Anharmonic lattice dynamics of solid potassium

H. R. Glyde
Department of Physics, University of Ottawa, Ottawa K1N 6N5, Canada

J. P. Hansen and M. L. Klein†
Laboratoire Physique Théorique des Liquides, Université Pierre et Marie Curie, 75230 Paris, France*
(Received 6 June 1977)

An interionic potential proposed by Dagens, Rasolt, and Taylor has been used in classical computer-simulation experiments on solid K at 162.5 and 311 K. Results for the dynamical structure factor $S(\vec{Q},\omega)$ are compared with lattice-dynamical calculations employing the self-consistent harmonic approximation plus cubic anharmonic corrections. The lattice-dynamical calculations are in good accord with the simulation data at the lower temperature but near the melting point the simulation data yield considerably broader phonons, in qualitative agreement with experimental neutron-scattering data. The anharmonic interference effect which couples the one-phonon $S_1(\vec{Q},\omega)$ to the multiphonon background is also discussed.

I. INTRODUCTION

The anharmonic properties of the simple alkali-metal potassium have been extensively studied over the past few years. The frequencies and lifetimes Γ^{-1} of the normal modes of vibrations or phonons have been measured over a wide range of temperature by inelastic neutron scattering.[1] The elastic constants[2] and other thermodynamic properties[3] are known up to the melting point. The volume dependence of the phonon frequencies has been studied[4] by neutron scattering as well as the interesting anharmonic interference effects which couple the one-phonon and multiphonon contributions to the dynamical structure factor.[5] This experimental work has in turn stimulated theoretical study.[1,6-8] Buyers and Cowley[1] calculated the shifts in phonon frequency and the phonon "linewidths" ($\sim 2\Gamma^{-1}$) due to anharmonicity using standard perturbation theory. Duesbury *et al.*[7] extended these calculations using the self-consistent harmonic (SCH) theory with contributions from cubic terms added (SCH + C). The resulting phonon frequencies compared well with the neutron data with little distinction between the self-consistent and perturbation methods within the experimental error. Near the melting point, however, the calculated phonon linewidths[1,7] were often a factor of 2 too small. This disagreement may signal that the remaining higher-order anharmonic contributions are important in potassium.

The melting temperature $T_m = 335$ K of solid potassium is about four times its Debye temperature. For this reason the lattice behaves classically at temperatures above $\sim \frac{1}{2} T_m$. Thus the powerful computer-simulation Monte Carlo (MC) and molecular dynamics (MD) methods can and have been used to study the thermodynamic[9] and time-dependent[10] properties. These simulation studies, which employed the effective ion-ion interaction potentials of Dagens, Rasolt, and Taylor (DRT), yielded elastic constants, phonon frequencies, and linewidths in good agreement with experiment up to the melting point. Thus the disagreement of the previously calculated linewidths while possibly due to use of less reliable interatomic potentials seems at least in part due to higher-order anharmonic effects. The purpose of the present work is therefore to investigate the magnitude of higher-order contributions in detail by direct comparison of the self-consistent phonon and computer-simulation studies.

Previous theoretical work[5,7] employed slightly different effective ion-ion potentials and state conditions that make explicit comparison with computer-simulation experiments somewhat indirect. Accordingly we have carried out self-consistent phonon calculations using the same (DRT) effective ion-ion potentials and state conditions as in the present extensions of previous molecular-dynamics studies.[10] In particular, we compare the dynamical structure factor $S(\vec{Q},\omega)$ as calculated by the MD and SCH + C methods for selected $\vec{Q}$ values at $T = 162.5$ K, $a = 5.2767$ Å and $T = 311$ K, $a = 5.333$ Å. Where appropriate, the SCH + C calculations include the interference contributions between the one-phonon and two-phonon components of $S(\vec{Q},\omega)$ and the two-phonon contributions to $S(\vec{Q},\omega)$. Section II outlines the theory and methods of computation. The results in Sec. III suggest that at one-half the melting point the two approaches give similar results. At higher temperatures, near melting, the MD data yield one-phonon groups considerably broader than those of the SCH + C theory indicating, we believe, the need to include higher-order anharmonic decay processes into existing phonon theories.

II. OUTLINE OF THE CALCULATIONS

A. Molecular dynamics

The molecular-dynamics computations followed the procedures used in previous studies of the fcc Lennard-Jones solid.[11] A solid of 432 particles each having mass 39.1 a.m.u. were initially arranged on a bcc lattice of appropriate lattice constant a. The classical equations of motion were solved using Verlet's finite-difference algorithm[12] with a time step of about 10^{-14} sec. Periodic boundary conditions were used to simulate the effect of an infinite crystal. Two runs of 10000 time steps each were carried out for $a = 5.2767$ Å and $T = 162.5$ K, and one run of 20000 time steps at $a = 5.333$ Å and $T = 311$ K. These state conditions correspond to roughly $\frac{1}{2}T_m$ and $\frac{9}{10}T_m$. The finite system size limits the number of independent phonon wave vectors along the [001] direction to six.

The ions interacted via the DRT potential which was truncated after eight shells of neighbors. This truncation, which takes place in a region where the potential is still oscillating with non-negligible amplitude, is necessary because of the finite system size. Previous studies of elastic constants[9] suggested that truncation at eight shells of neighbors (a distance $\sim 2.5a$) gave a reasonable compromise between truncation errors and computational time. Studies of the truncation dependence of the harmonic phonon frequencies showed that only the frequencies of the slowest transverse branch $T_1[110]$, were significantly affected by the truncation (by $\sim 7\%$). Duesbury and Taylor[13] have recently shown how to treat a long-range oscillating potential using Ewald-type methods and in fact the DRT potential provides phonon frequencies in excellent agreement with recent measurements of the $T_1[110]$ branch.[14]

The raw MD data were stored every fourth step on a tape and subsequently used to compute statistical averages. A few equilibrium properties such as the internal energy, the pressure, the mean square amplitude of vibration of an ion, and the isotropic pair distribution function $g(r)$ were also calculated.

The main effort went into the computation of the dynamical structure factor $S(\vec{Q}, \omega)$. This is the Fourier transform with respect to time

$$S(\vec{Q}, \omega) = \int dt\, e^{i\omega t} F(\vec{Q}, t)$$

of the correlation function

$$F(\vec{Q}, t) = (1/N)\langle \rho(\vec{Q}, t)\rho(-\vec{Q}, 0)\rangle$$

of the particle density operator

$$\rho(\vec{Q}, t) = \sum_i \exp[-i\vec{Q}\cdot\vec{r}_i(t)].$$

Here the sum runs over the N atoms in the solid whose positions at time t are given by $\vec{r}(t) = \vec{R} + \vec{u}(t)$, where $\vec{u}(t)$ is the displacement from the lattice point R. The angular brackets denote the statistical average that is evaluated using the MD data. Since our computations are purely classical they violate the well-known detailed balance condition

$$S(\vec{Q}, -\omega) = e^{-\beta\hbar\omega} S(\vec{Q}, \omega).$$

In the following comparisons of the MD results with lattice dynamical calculations we use Schofield's ansatz[15] to correct the MD data.

The one-phonon approximation to the intermediate scattering function is

$$F_1(\vec{Q}, t) = (1/N)\langle \tilde{\rho}(\vec{Q}, t)\tilde{\rho}(-\vec{Q}, 0)\rangle,$$

where

$$\tilde{\rho}(\vec{Q}, t) = d(Q)\sum_i [-i\vec{Q}\cdot\vec{u}_i(t)]\, e^{i\vec{Q}\cdot\vec{R}_i}$$

and

$$d(Q) = \langle e^{i\vec{Q}\cdot\vec{u}}\rangle \simeq e^{W_0},$$

where $W_0 = -\frac{1}{6}|\vec{Q}|^2\langle u^2\rangle$. In the MD calculations both $F(\vec{Q}, t)$ and $F_1(\vec{Q}, t)$ can be evaluated with equal facility[11] providing a test of the "phonon expansion" of $S(\vec{Q}, \omega)$. The corresponding dynamical structure factors obey the f sum rules[16]

$$\int_{-\infty}^{\infty} \frac{d\omega}{2\pi}\omega^2 S(\vec{Q}, \omega) = kT\frac{Q^2}{2m},$$

$$\int_{\infty}^{\infty} \frac{d\omega}{2\pi}\omega^2 S_1(\vec{Q}, \omega) = kT\frac{Q^2}{2m}d^2(Q).$$

We have evaluated $S(\vec{Q}, \omega)$ for selected $\vec{Q}$ values along the principal symmetry directions. The MD computations satisfy the sum rules within about 10%. Errors arise from several sources, not the least of which is related to the long-time behavior of $F(\vec{Q}, t)$. Because of the finite length of our computations, sharp phonon groups will be artificially broadened by the time truncation of $F(\vec{Q}, t)$, adding a width of $\sim(0.03-0.05)$ THz to the phonon groups shown in Sec. III. The arbitrariness of separating $F(\vec{Q}, t)$ from the long-time noise introduces uncertainties in the broader phonons. We also employed the so-called "direct method" of computing $S(\vec{Q}, \omega)$ and intercomparison of the two methods is useful in estimating uncertainties. Koehler and Lee[17] have discussed the general problem of best using MD methods to study dynamical properties. The implementation of their ideas, however, does not seem feasible for our relatively small system size.

B. Self-consistent phonon dynamics

The procedures used to calculate $S(\vec{Q}, \omega)$ in the SCH+C approximation follow previous work[7] except that the DRT potential[6] was employed. The usual phonon expansion of $S(\vec{Q}, \omega)$ yields[16]

$$S(\vec{Q}, \omega) = S_0(\vec{Q}, \omega) + S_1(\vec{Q}, \omega) + S_{12}(\vec{Q}, \omega) + S_2(\vec{Q}, \omega) + \cdots .$$

The S_0 is the static Bragg scattering of no interest here, while S_1 and S_2 are the contributions in which one and two phonons are created (or destroyed), respectively. The S_{12} is the purely anharmonic interference contribution which couples the sharply peaked single-phonon process to the two-phonon process which usually forms a generally uniform background. The S_1 and S_{12} can be combined to yield

$$S_p(\vec{Q}, \omega) = S_1(\vec{Q}, \omega) + S_{12}(\vec{Q}, \omega).$$

The dominant terms of $S_p(\vec{Q}, \omega)$ can be expressed in the form[5, 18]

$$S_p(\vec{Q}, \omega) = S_1(\vec{Q}, \omega)\left[1 - 2\left(A + \frac{B(\Omega_{q\lambda}^2 - \omega^2)}{2\omega_{q\lambda}\Gamma_{q\lambda}}\right)\right],$$

where A and B are approximately frequency-independent constants, $\Omega_{q\lambda}^2 = \omega_{q\lambda}^2 + 2\omega_{q\lambda}\Delta_{q\lambda}$ is the anharmonic one-phonon frequency, and $\omega_{q\lambda}$ is the SCH frequency.

From $S_p(\vec{Q}, \omega)$ above we see there are two distinct types of interference contributions. The first, $S_{12}^A(\vec{Q}, \omega)$, is essentially a constant $(-2A)$ times $S_1(\vec{Q}, \omega)$ and hence adds or subtracts an intensity proportional to $S_1(\vec{Q}, \omega)$ depending on the sign of A. The sign of A changes as $\vec{Q}$ passes through a Bragg vector, or the midpoint between two Bragg vectors, causing an "oscillation" in the magnitude of $S_p(\vec{Q}, \omega)$ about $S_1(\vec{Q}, \omega)$ with $\vec{Q}$. The second, $S_{12}^B(\vec{Q}, \omega)$, is asymmetric about $\Omega_{q\lambda}$, the frequency of the phonon involved in the one-phonon process. This has the effect of raising or lowering the apparent multiphonon background on each side of $S_1(\vec{Q}, \omega)$ and for broad $S_1(\vec{Q}, \omega)$ can shift the peak position of $S_p(\vec{Q}, \omega)$ away from that of $S_1(\vec{Q}, \omega)$. The sign of B "oscillates" with Q as does A.

Higher-order interference contributions have been discussed in the literature in the context of x-ray diffuse scattering[19] but we shall not consider these here. To the present level of approximation, the interference terms vanish for zone-boundary phonons. Thus for zone-boundary phonons we compare S_1(MD) and S_1(SCH+C) to test the usual theory of single-phonon dynamics. For other phonons comparison of the full S(MD) and $S_p + S_2$(SCH+C) will test the importance of multiphonon and higher interference contributions.

III. RESULTS

A. Equilibrium properties

Before entering the detailed discussion of the dynamical structure factors we report a few results on the equilibrium properties (for the truncated potential) in Table I. The MD elastic constants c_{11} and c_{44} were obtained from the frequencies of the phonons of smallest wave vector in the [001] direction. There is good agreement between the MC and MD values near the melting point as well as at the lower temperatures (not shown explicitly). We see that the c_{44} elastic constants calculated from the SCH+C approximation discussed in Sec. II B are significantly larger indicating that the SCH+C transverse [001] phonon frequencies at low Q are ~(5–10)% too large. This branch is particularly interesting since the frequency shifts due to the cubic and quartic anharmonic terms are both of the same sign (negative). Hence any omitted higher anharmonic shifts may be expected to be negative and additive. The simulation data are in good agreement with experiment.[2]

In Fig. 1 we show the spherically averaged radial distribution functions $g(r)$. These are of interest since scattering from small crystallites can be used to obtain $g(r)$.[20] Although eight shells of neighbors are included in the calculations, the thermal motion smears these into only four apparent peaks.

TABLE I. Some calculated equilibrium properties of potassium.

	$T = 311$ K, $a = 5.333$ Å				$T = 162.5$ K, $a = 5.2767$ Å		
	(MD)	(MC)[a]	(SCH)	(SCH+C)	(MD)	(SCH)	(SCH+C)
E/NkT	−3.35	−3.46	−3.53	···	···	−9.01	···
pV/NkT	7.2	7.0	···	···	···	···	···
c_{11} (kbar)	37.4	37.1	41.6	36.5	40.0	43.8	39.4
c_{44} (kbar)	18.3	18.5	24.2	20.6	24.4	26.9	25.2
$\langle u^2\rangle^{1/2}/R_{NN}$	0.162	0.20 ± 0.02	0.136	···	0.106	0.0984	

[a] Results from Ref. 9 for a 250-particle system at $T = 308$ K, $a = 5.333$ Å.

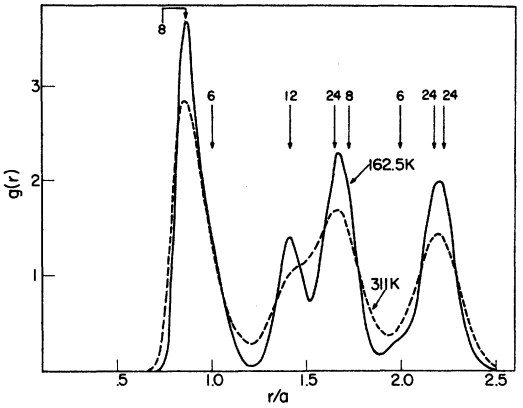

FIG. 1. Spherically averaged pair distribution functions $g(r)$ for solid K at 162.5 K (solid line) and 311 K (dashed line). The position and number of neighbors at a given distance r are indicated by the arrows and numbers, respectively.

B. Dynamical structure factors

We first display a few selected MD results to illustrate the overall behavior of $S(\vec{Q}, \omega)$ as the temperature is increased from 0.5 to 0.9 of the melting temperature. Figure 2 shows the H_{15} phonon at wave vector $\vec{Q}^* = \vec{Q}a/2\pi = (2, 2, 1)$. At 162.5 K the peak occurred at 2.05 THz and had a full width at half-maximum (FWHM) of 0.1 THz. This shifted and broadened substantially at 311 K (1.88 THz; FWHM ~ 0.25 THz). Figure 3 shows $S(\vec{Q}, \omega)$ for the transverse phonon at $Q^* = (2, 2, \frac{2}{3})$. This

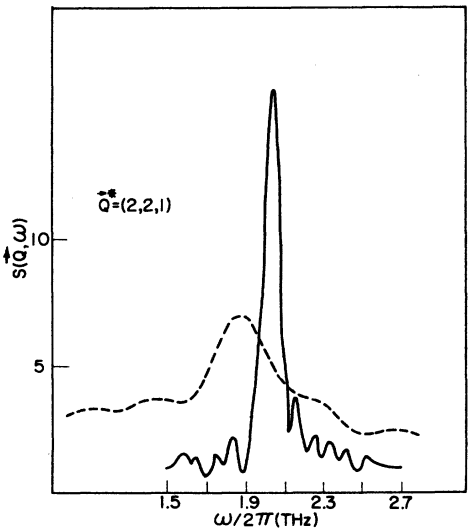

FIG. 2. Molecular-dynamics calculation of the temperature dependence of $S(\vec{Q}, \omega)$ for $\vec{Q}^* = \vec{Q}a/2\pi = (2, 2, 1)$. This is the zone boundary, H_{15} phonon for 162.5 K (solid line) and 311 K (dashed line).

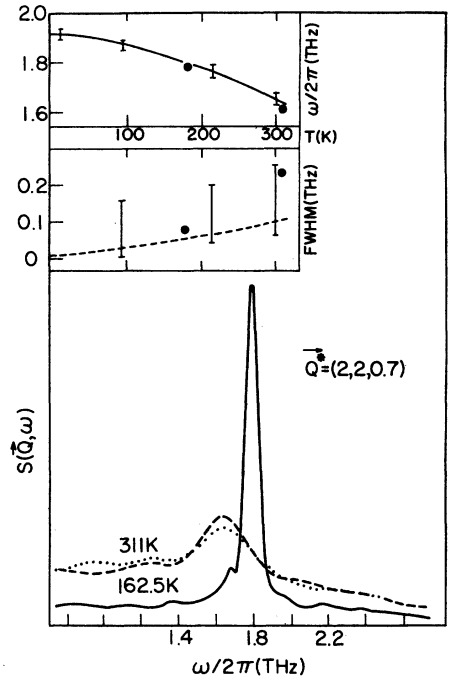

FIG. 3. MD $S(\vec{Q}, \omega)$ for the transverse polarization at $\vec{Q}^* = (2, 2, \frac{2}{3})$. The solid line corresponds to 162.5 K, the dashed line to 311 K. The dotted line is the 311-K result averaged over one-half of the MD run. The inset figures show the comparison of MD data (dots) with the experimental data (solid line and error bars) of Ref. 1. A previous calculation (Ref. 7) of the FWHM is shown as a dashed line.

phonon is close to that observed and shown explicitly by Buyers and Cowley[1] [$Q^* = (2, 2, 0.7)$]. We see from the insets of Fig. 3 that at both temperatures the MD phonon peak positions and FWHM agree well with the observed values. The shape of $S(\vec{Q}, \omega)$ at 311 K, including the multiphonon background, resembles closely the observed phonon group.[1]

Meyer et al.[5] measured $S(\vec{Q}, \omega)$ for longitudinal polarization along [110] for $Q^* = (\zeta, \zeta, 0)$, $\zeta = 1.8$, 2.2, 2.8, and 3.2 at $T = 4.5$, 99, and 150 K. From an analysis of their data they were able to identify both the anharmonic interference contributions, S_{12}^A and S_{12}^B which are symmetric and asymmetric about the one-phonon peak, respectively. The integrated intensity in the one-phonon region, affected by S_{12}^A, and the slope of the background, affected by S_{12}^B, were observed to "oscillate" as $\vec{Q}$ crossed a Bragg vector or a midpoint between two Bragg vectors. Figure 4 illustrates these interference contributions, as calculated using the SCH + C approximation of Sec. II B, for potassium at 311 K by comparing $S_p = S_1 + S_{12}^A + S_{12}^B$ with S_1 alone. The S_{12}^A creates an oscillation in the intensity of S_p about S_1 while S_{12}^B appears as an os-

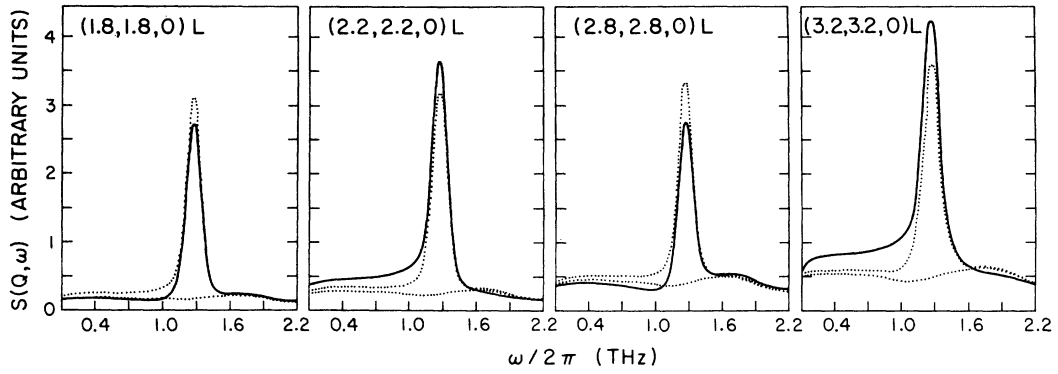

FIG. 4. Interference effect in $S(\vec{Q},\omega)/Q^2d^2(Q)$ for $Q^*=(\zeta,\zeta,0)$, $\zeta=1.8$, 2.2, 2.8, 3.2 calculated using the SCH+C theory at 311 K. The $S_2(\vec{Q},\omega)$ is the lower dotted line, $S_1(\vec{Q},\omega)+S_2(\vec{Q},\omega)$ is the peaked dotted line and $S_p(\vec{Q},\omega)+S_2(\vec{Q},\omega)$, including the one–two-phonon interference contribution, is the full line. Each $S(\vec{Q},\omega)$ is folded with a Gaussian with a FWHM of 0.13 THz.

cillation in the background, chiefly on the low-frequency side of the one-phonon peak.

Figure 5 shows the computer simulation results for $S(\vec{Q},\omega)$ for similar phonons, $\vec{Q}^*=(\zeta,\zeta,0)$, $\zeta=\frac{11}{6}$, $\frac{13}{6}$, $\frac{17}{6}$, and $\frac{19}{6}$ at 311 K. The data, as the SCH+C results, were convoluted with a Gaussian with a FWHM of 0.13 THz to simulate a finite neutron-spectrometer energy-resolution width. The interference effect manifests itself most strongly by the large intensity changes on the low-frequency side of the one-phonon peak. A shift in peak position is also visible for the highest $\vec{Q}$ in Fig. 5 which is not visible in the SCH+C case. A shift in peak position by S_{12}^{δ} is possible only if the phonon group has significant intrinsic width. This shift illustrates the larger intrinsic width calculated in the MD simulation. In Fig. 5 we also see that the zone boundary $\vec{Q}^*=(2.5, 2.5, 0)L$ phonon is sufficiently broad that it is barely visible above the multiphonon background. This perhaps explains why no results were reported experimentally for this phonon at elevated temperatures.

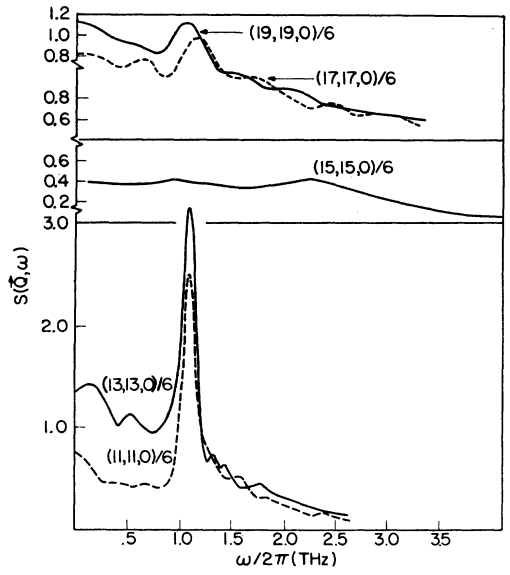

FIG. 5. Interference effect in the MD $S(\vec{Q},\omega)$ for $Q^*=(\zeta,\zeta,0)$, $\zeta=\frac{11}{6}$, $\frac{13}{6}$, $\frac{15}{6}$, $\frac{17}{6}$, $\frac{19}{6}$ at 311 K folded with a Gaussian with a FWHM of 0.13 THz.

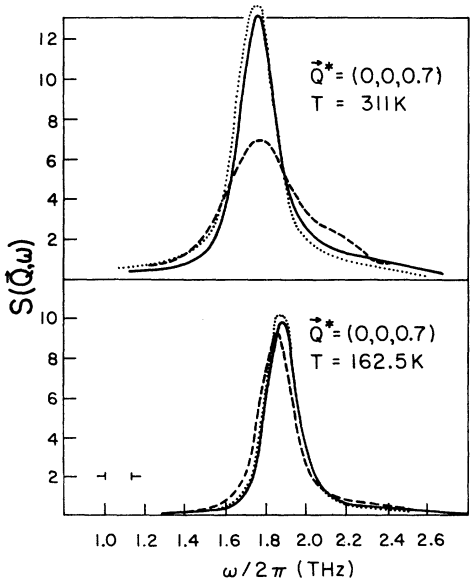

FIG. 6. Comparison of MD simulation and lattice dynamic, SCH+C theory. The lower graph is 162.5 K; the upper, 311 K. The dashed curves are the MD $S(\vec{Q},\omega)$ for $\vec{Q}^*=(0,0,\frac{2}{3})$. The dotted lines are $S_1(\vec{Q},\omega)$ and the full lines are $S_p(\vec{Q},\omega)$ for the SCH+C theory at $\vec{Q}^*=(0,0,0.7)$. Both the MD and SCH+C $S(\vec{Q},\omega)$ are convoluted with a Gaussian with a FWHM of 0.13 THz.

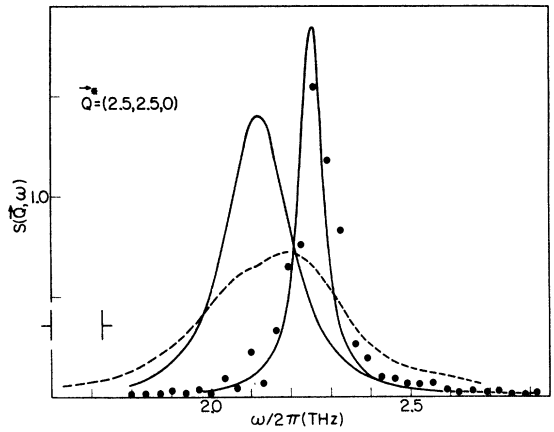

FIG. 7. Comparison of the MD simulation with the SCH+C theory $S_1(\vec{Q},\omega)$ for the longitudinal phonon at $\vec{Q}^* = (2.5, 2.5, 0)$. The dots are MD data at 162.5 K, the dashed the MD data at 311 K convoluted with a Gaussian with a FWHM of 0.13 THz. The full lines are the SCH+C $S_1(\vec{Q},\omega)$ with the 311 K result on the left-hand side similarly convoluted.

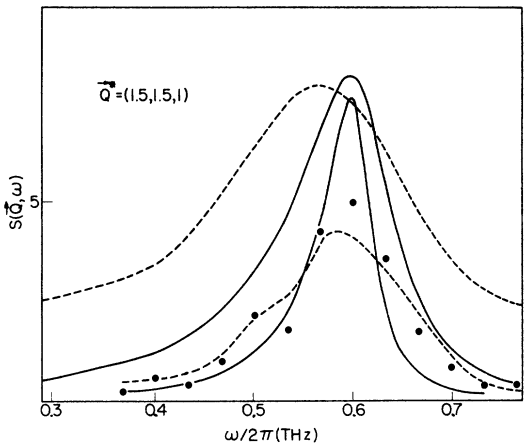

FIG. 9. Comparison of the MD and SCH+C theory $S(\vec{Q},\omega)$ for the slow transverse phonon at $\vec{Q}^* = (1.5, 1.5, 1)$. At 162.5 K the dots show the MD $S(\vec{Q},\omega)$ calculated by the "direct method" and the dashed curve the MD $S(\vec{Q},\omega)$ calculated from the time-correlation function. The upper dashed curve is the corresponding MD result at 311 K. The full curves are the $S_1(\vec{Q},\omega)$ by SCH+C.

We now compare some selected phonon groups as calculated by MD with the predictions of the lattice-dynamic theory, SCH+C in order to identify any differences. Figure 6 compares the MD data for $S(\vec{Q},\omega)$, $\vec{Q}^* = (2/3, 0, 0)L$ with the SCH+C calculation of $S_1(\vec{Q},\omega)$ and $S_\rho(\vec{Q},\omega)$ for $\vec{Q}^* = (0.7, 0, 0)L$. The interference effect seems primarily responsible for the asymmetry in the one-phonon peak. There is good agreement at 162.5 K between the two calculations; the small difference in peak position and height can be ascribed to the different wave vectors used in each calculation. At 311 K the MD one-phonon group is broader and more asymmetric than the SCH+C result. We believe these differences are due to higher-order anharmonic effects.

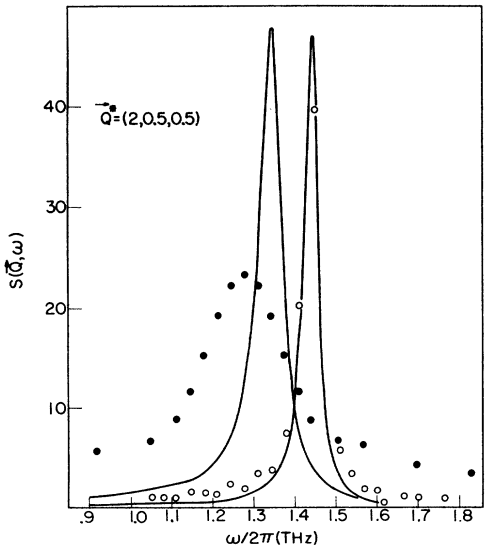

FIG. 8. Comparison of the MD and SCH+C theory $S(\vec{Q},\omega)$ for the fast transverse phonon at $\vec{Q}^* = (2, 0.5, 0.5)$. The open circles are the MD results at 162.5 K, the full circles the MD at 311 K. The full lines are $S_1(\vec{Q},\omega)$ by SCH+C.

To identify the differences more closely, Fig. 7 shows $S_1(\vec{Q},\omega)$ alone for $\vec{Q}^* = (2.5, 2.5, 0)L$ calculated by MD and SCH+C methods. At 162.5 K there is relatively close accord although the MD $S_1(\vec{Q},\omega)$ peaks at a slightly higher energy. At 311 K the simulation phonon group is considerably broader than the SCH+C theory result. This comparison of $S_1(\vec{Q},\omega)$ alone shows that the difference in one-phonon width is due to anharmonic terms damping the single phonon in the absence of possible complications from multiphonon or interference effects.

Figure 8 shows the highest-frequency transverse T_2 phonon at the [110] zone boundary. The simulated $S(\vec{Q},\omega)$ data are for $\vec{Q}^* = (2, 0.5, 0.5)$. At 162.5 K there is relatively close agreement between the MD data and the SCH+C theory (S_1+S_2). However at 311 K significant differences are apparent with the MD data yielding a substantially broader phonon having a somewhat smaller frequency. The latter is not unexpected since at small wave vector the slope of this branch yields the c_{44} elastic constants given in Table I. The

TABLE II. Phonon frequencies, $\omega/2\pi$ (in THz), for $q=(2\pi/a)(0.5, 0.5, 0)$.

Model \ Polarization	L Temperature (K)			T_1 Temperature (K)			T_2 Temperature (K)		
	5	162.5	311	5	162.5	311	5	162.5	311
QH	2.36	2.27	2.16	0.55	0.52	0.50	1.52	1.50	1.46
SCH		2.32	2.25		0.62	0.65		1.48	1.42
SCH+C		2.26	2.12		0.60	0.59		1.43	1.33
MD		2.28	2.17		0.59	0.56		1.43	1.27
Expt.	2.40 ± 0.01 [a]			0.555 [b] ±0.008	0.54 [c] ±0.03	0.52 [c] ±0.03	1.50 [a] ±0.02		1.30 [d] ±0.06

[a] Cowley *et al.*, Ref. 23.
[b] Dolling and Meyer, Ref. 14.
[c] Buyers and Cowley, Ref. 1.
[d] Interpolated from Σ_3 branch and P_4, Ref. 1.

much larger background in the MD simulation data may be due, in part, to the S_{13} interference contribution which does not vanish at zone boundaries.[19]

Finally in Fig. 9 we show the slow transverse T_1 phonon at the [110] zone boundary. The MD data $S(\vec{Q}, \omega)$ are for $\vec{Q}^* = (1.5, 1.5, 1)$. Again the agreement between the SCH+C, S_1+S_2, and the MD $S(\vec{Q}, \omega)$ is reasonable at 162.5 K, but at 311 K the MD simulation yields a substantially broader phonon group. Figures 7–9 serve to demonstrate the differences in one-phonon widths calculated by theory and simulation. The difference in the one-phonon frequencies calculated in various approximations, including the quasiharmonic (QH) theory, is displayed in Table II.

IV. SUMMARY

The MD simulation and analytic SCH+C theory are in reasonable agreement for $S(\vec{Q}, \omega)$ at modest $\vec{Q}$ values at about one-half the melting temperature of potassium. One might then expect lattice-dynamic theories to apply with confidence for calculation of dynamic and thermodynamic properties in this range. At higher temperatures, near melting, there are often significant differences between the MD and SCH+C theory particularly in the phonon group widths. The FWHM of the MD $S(\vec{Q}, \omega)$ is often about twice that calculated by the SCH+C theory with MD results agreeing well with experiment.[1] This difference explains a discrepancy between the SCH+C theory and experiment noted earlier[1,7] and points to the importance of including higher anharmonic terms beyond the cubic in calculating phonon lifetimes. The phonon frequencies calculated by the two methods generally agree within a few percent.

Near melting we believe that the differences between SCH+C and MD data are significant. Thus at the present level of application, self-consistent-phonon theories do not provide a complete description of the one-phonon response. Some attempts have been made to extend and improve phonon theories[21,22] and perhaps the MD data presented in this paper will stimulate further work along these lines.

ACKNOWLEDGMENT

One of us (H.R.G.) thanks the NRC (Canada)–CNRS (France) exchange program for their support of this collaboration.

*Laboratoire Associé au Centre National de la Recherche Scientifique.
†Permanent address: Chemistry Div., National Research Council of Canada, Ottawa, K1A 0R6, Ontario, Canada.

[1] W. J. L. Buyers and R. A. Cowley, Phys. Rev. 180, 755 (1969).
[2] G. Fritsch and H. Bube, Phys. Status Solidi A 30, 571 (1975).
[3] D. R. Schouten and C. A. Swenson, Phys. Rev. B 6, 2175 (1974).
[4] J. Meyer, G. Dolling, J. Kalos, C. Vettier, and J. Paureau, J. Phys. F 6, 1899 (1976).
[5] J. Meyer, G. Dolling, R. Scherm, and H. R. Glyde, J. Phys. F 6, 943 (1976).
[6] L. Dagens, M. Rasolt, and R. Taylor, Phys. Rev. B 11, 2726 (1975).
[7] M. S. Duesbury, R. Taylor, and H. R. Glyde, Phys. Rev. B 8, 1372 (1973).
[8] R. Taylor and H. R. Glyde, J. Phys. F 6, 1915 (1976).
[9] S. S. Cohen and M. L. Klein, Phys. Rev. B 12, 2984 (1975).
[10] J. P. Hansen and M. L. Klein, Solid State Commun. 20, 771 (1976).
[11] J. P. Hansen and M. L. Klein, Phys. Rev. B 13, 878 (1976).
[12] L. Verlet, Phys. Rev. 159, 98 (1967).
[13] M. S. Duesbury and R. Taylor, J. Phys. F 7, 47 (1977).
[14] G. Dolling and J. Meyer, J. Phys. F 7, 775 (1977).
[15] P. Schofield, Phys. Rev. Lett. 4, 239 (1960).

[16]V. Ambegaokar, J. Conway, and G. Baym, in *Lattice Dynamics*, edited by R. F. Wallis (Pergamon, New York, 1965), p. 261; W. J. L. Buyers and R. A. Cowley, J. Phys. C 2, 2262 (1969).
[17]T. R. Koehler and P. A. Lee, J. Comp. Phys. 22, 319 (1976).
[18]H. R. Glyde, Can. J. Phys. 52, 2281 (1974).
[19]J. S. Reid, in *Phonons*, edited by M. A. Nusimovici (Flammarion, Paris, 1971), p. 134.
[20]R. B. Schierbrock and G. Fritsch, Phys. Lett. A 48, 151 (1974).
[21]H. Horner, in *Dynamical Properties of Solids*, edited by A. A. Maradudin and G. K. Horton (North-Holland, Amsterdam, 1974), p. 450.
[22]L. B. Kanney and G. K. Horton, Phys. Rev. Lett. 34, 1565 (1974).
[23]R. A. Cowley, A. D. B. Woods, and G. Dolling, Phys. Rev. 150, 487 (1966).